Research Article

Linrun Li, Suohe Yang, Haibo Jin*, Guangxiang He, Xiaoyan Guo, and Lei Ma

The experimental study on the air oxidation of 5-hydroxymethylfurfural to 2,5-furandicarboxylic acid with Co–Mn–Br system

https://doi.org/10.1515/gps-2023-0116
received June 29, 2023; accepted October 9, 2023

Abstract: 2,5-Furandicarboxylic acid (FDCA), an eco-friendly biomass resource capable of replacing petroleum-based fuels, is gaining increasing popularity. In this article, 2,5-FDCA was prepared by liquid-phase oxidation of the sustainable precursor 5-hydroxymethylfurfural using the Co–Mn–Br catalyst system. The effects of catalyst concentration, catalyst ratio, reaction temperature, reaction time, reaction pressure, and solvent ratio on the reaction of FDCA were investigated. The products are subjected to qualitative and quantitative analyses using high-performance liquid chromatography, infrared spectroscopy, and hydrogen nuclear magnetic spectroscopy. Moreover, considering the loss of catalytic liquid, the suitable reaction conditions were determined as follows: n(Co)/n(Mn)/n(Br) = 1/0.04/0.5, n(HMF)/n(HAC) = 0.05, reaction temperature of 170°C, reaction pressure of 2 MPa, reaction time 40 min, and airflow rate 1.0 L·min^{-1}. Under these conditions, the yield of the product is 86.01%, the purity is 97.53%, and the loss of the catalytic liquid is about 5.63%, which is at an ideal level and provides a good basis for the recovery of the subsequent catalytic liquid and multiple cycle reactions. Through the optimization of the existing process, the use of noble metal catalysts has been reduced, and the recycling of catalytic liquid has also reduced the consumption of catalysts. This advancement marks a significant stride toward sustainable development in the green chemical industry.

*** Corresponding author: Haibo Jin,** School of New Materials and Chemical Engineering, Beijing Institute of Petrochemical and Technology, Beijing 102617, China; Beijing Key Laboratory of Fuels Cleaning and Advanced Catalytic Emission Reduction Technology, Beijing 102617, China, e-mail: jinhaibo@bipt.edu.cn

Linrun Li, Suohe Yang, Guangxiang He, Xiaoyan Guo, Lei Ma: School of New Materials and Chemical Engineering, Beijing Institute of Petrochemical and Technology, Beijing 102617, China; Beijing Key Laboratory of Fuels Cleaning and Advanced Catalytic Emission Reduction Technology, Beijing 102617, China

Keywords: 5-hydroxymethylfurfural, 2,5-furandicarboxylic acid, Co–Mn–Br, liquid-phase oxidation

1 Introduction

As the consumption of non-renewable resources continues to rise, the copious release of gases such as CO, CO_2, SO_2, and others has contributed to the escalation of environmental pollution and intensifies the greenhouse effect in the atmosphere, exacerbating the energy crisis. The pursuit of sustainable and eco-friendly alternatives has become an urgent priority [1]. Therefore, there is a growing preference for green biomass resources, which offer abundant content and minimal environmental pollution impact [2]. The substitution of biomass resources for fossil resources presents a viable solution to mitigate the environmental issues associated with fossil fuel combustion and alleviate the energy crisis [3].

2,5-Furandicarboxylic acid (FDCA), recognized as an essential green bio-based chemical [4,5], was included among the high-value-added bio-based chemicals by the U.S. Department of Energy in 2004 [6]. Polycondensation of FDCA with ethylene glycol (EG) enables the production of high-performance bio-based polyester materials, such as polyethylene 2,5-furan dicarboxylate (PEF). Compared with polyethylene terephthalate (PET), PEF is superior to PET in terms of tensile strength, Young's modulus, gas barrier properties, thermal stability, and mechanical properties. Additionally, PEF offers the advantages of environmental sustainability and renewability [7–9]. FDCA can not only be used as the upstream monomer of new polyester materials but also be widely used in food materials, medical materials, aviation materials, and other fields [10–16]. Its diverse applications make it a subject of significant research interest. Therefore, it is necessary to develop sustainable, eco-friendly, and heterogeneous catalytic methods for the preparation of green biomass and its derivatives under mild reaction conditions [17].

The liquid-phase catalytic oxidation of 5-hydroxymethylfurfural (HMF) to FDCA synthesis can be divided into biosynthesis and chemical synthesis. In the biosynthesis method [18], the preparation process involving biological enzyme catalyst is complex, and the subsequent product purification is challenging. The chemical synthesis method utilizing the glycolic acid method [19] for FDCA preparation encounters issues with unfriendly reaction conditions, such as the EG rearrangement, resulting in low yields. As a consequence, its large-scale industrial applications remain limited. The furfural (furoic acid) method for FDCA production [20,21], utilizing green and environmentally friendly starting materials, faces challenges due to the presence of numerous isomers, making separation and purification difficult. Moreover, the recovery and treatment of by-product salts pose complexities, rendering it impractical. However, using HMF as raw material, the preparation of FDCA by liquid-phase oxidation is favored because of its simple process and excellent yield and purity. This process builds upon the Mid-Century liquid-phase oxidation process and demonstrates suitability for industrial production. In the single-pot operation of heterogeneous catalytic systems, the separation and purification of intermediates can be significantly eliminated and the formation of unwanted by-products can be prevented [22–24].

Eastman company [25] used the MC production process, which involves the liquid-phase air catalytic oxidation of furfural derivatives method such as 5-methyl-2-furfural and 5-ethyl hydroxymethyl-2-furfural, to prepare FDCA using the Co–Mn–Br catalytic system. Furanix Technologies B.V. [26] also employed the Co–Mn–Br catalytic system, but they used a mixture of one or more of these compounds as raw materials at a specific temperature and pressure. These furfural derivatives included 5-HMF, 5-methyl furfural, 5-methylfuroic acid, and 2,5-dimethylfuran. The solvent used in this process was a mixture of acetic acid and water. Canon Co. in Japan [27] has also developed a method for producing FDCA by liquid-phase catalytic oxidation of 5-HMF using the Co–Mn–Br catalytic system. At the same time, this method proposed controlling the water content in the solution to avoid catalyst deactivation and reduce combustion side reactions to improve the FDCA yield. Therefore, the Co–Mn–Br homogeneous catalytic oxidation system serves as a valuable reference and provides guidance for the large-scale preparation of FDCA.

In this study, FDCA was synthesized by liquid-phase oxidation of HMF. The effects of catalyst concentration, ratio, temperature, reaction time, pressure, and solvent ratio on the yield of oxidation reaction and the loss of reaction solvent were investigated. Through the investigation of the process conditions, the more suitable reaction conditions were obtained. Additionally, the potential for recycling the catalytic liquid was investigated, offering valuable insights for future industrial applications.

2 Experimental part

2.1 Reagents and instruments

The following reagents were used in the experiments: 5-HMF (98% purity), 2,5-FDCA (99% purity), glacial acetic acid, cobalt acetate tetrahydrate, manganese acetate tetrahydrate, hydrobromic acid (48% aqueous solution), trifluoroacetic acid, and methanol. All were obtained from Meryer (Shanghai) Chemical Technology Co. Ltd. Deionized water was used throughout the experiments.

The following experimental instruments were used: high-performance liquid chromatography (Agilent 1290), Fourier transform infrared spectrometer (Thermo Scientific Nicolet iS20), ultrasonic cleaning machine (PS-100A), electronic balance (MP4002), and high-speed centrifuge.

2.2 Experimental apparatus and methods

The experiment was carried out in a titanium reactor, as shown in Figure 1. The catalyst, raw material, and reaction solvent were mixed in the specified proportion, heated, and dissolved. The resulting mixture was then added to the titanium reactor through the feed port. Nitrogen gas was introduced to replace the air inside the reactor, while leak detection was performed simultaneously. The system pressure was adjusted, and the reaction mixture was heated and stirred. The airflow was measured using a mass flowmeter. After the completion of the reaction, the reactor was washed with glacial acetic acid to obtain a mixed solution containing FDCA. The solid–liquid separation was employed to separate the oxidation product FDCA, while the recovered catalytic liquid could be recycled for subsequent reactions.

2.3 Product analysis method

The product was identified as FDCA by infrared spectrum analysis after drying, and the infrared spectrum of the product is shown in Figure 2. In Figure 2a, the characteristic peaks at 1,691 and 1,572 cm^{-1} are the product marker peaks. The characteristic absorption peak at 1,691 cm^{-1}

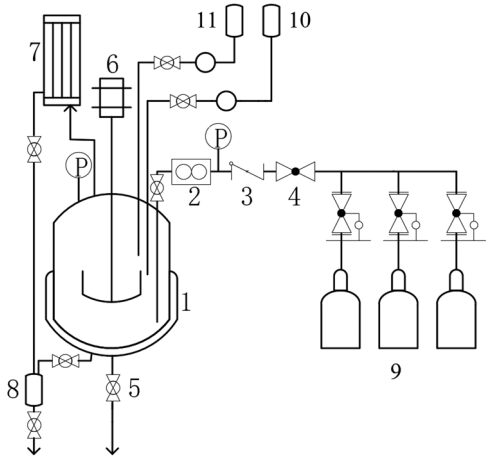

Figure 1: Reactor plant. 1. Reactor, 2. Mass flow meter, 3. One-way valve 4. Ball valve 5. Screw valve 6. Stirrer 7. Condenser 8. Tank 9. Gas cylinder 10. Feed port 11. Catalyst feed port.

corresponds to the C═O stretching vibration of the carboxylic acid group, confirming the absorption peak of carboxylic acid. The absorption peak at 1,572 cm^{-1} represents the C═C stretching vibration of the furan ring, further supporting the identification of FDCA. It is consistent with the Fourier transform infrared (FTIR) spectra of the standard product (as shown in Figure 2b).

Figure 3 is the H^1 NMR spectrum of the oxidation product. As shown in Figure 3a, the spectrum reveals two single peaks of H at the chemical shift δ 13.60, corresponding to H7 and H9 on the carboxyl group. Additionally, there are two single peaks of H at the chemical shift δ 7.28, representing H2 and H3 on the furan ring. Figure 3b is the H^1 NMR spectra of FDCA, based on the hydrogen nuclear magnetic analysis, the structure of the oxidation product H was confirmed to be consistent with FDCA.

3 Results and discussion

3.1 Influence of total catalyst concentration on reaction

The effects of different catalyst concentrations on the loss of oxidation products and catalytic liquid are illustrated in Figure 4. From Figure 4, with the increase of catalyst concentration, the yield and purity of the product increased first and then decreased, while the loss of catalytic liquid exhibits an upward trend. This is because, with the increase of Co–Mn–Br catalyst concentration, the active free radicals in the oxidation reaction gradually increase, accelerating the oxidation reaction and facilitating the conversion of substrate HMF to FDCA.

However, when the catalyst concentration exceeds a certain threshold, the excessive catalytic concentration leads to intensify the condensation of intermediate products and side reactions, resulting in reduced product yield and purity. However, the increase in catalyst concentration can accelerate the initiation of free radical chain reaction, thus accelerating the oxidation reaction. However, if the concentration is too high, the free radicals are too active, which are easy to attack the furan ring, and then trigger the ring opening, so that the substrate is deeply oxidized,

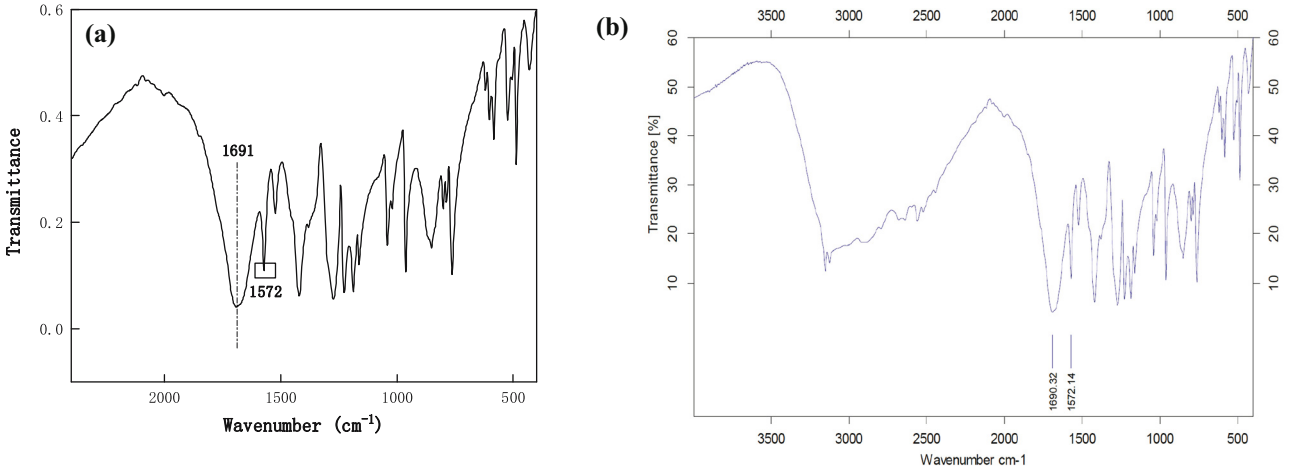

Figure 2: FTIR spectra of FDCA. Figure 2a is the infrared spectrum of product. Figure 2b is the infrared spectrum of standard sample.

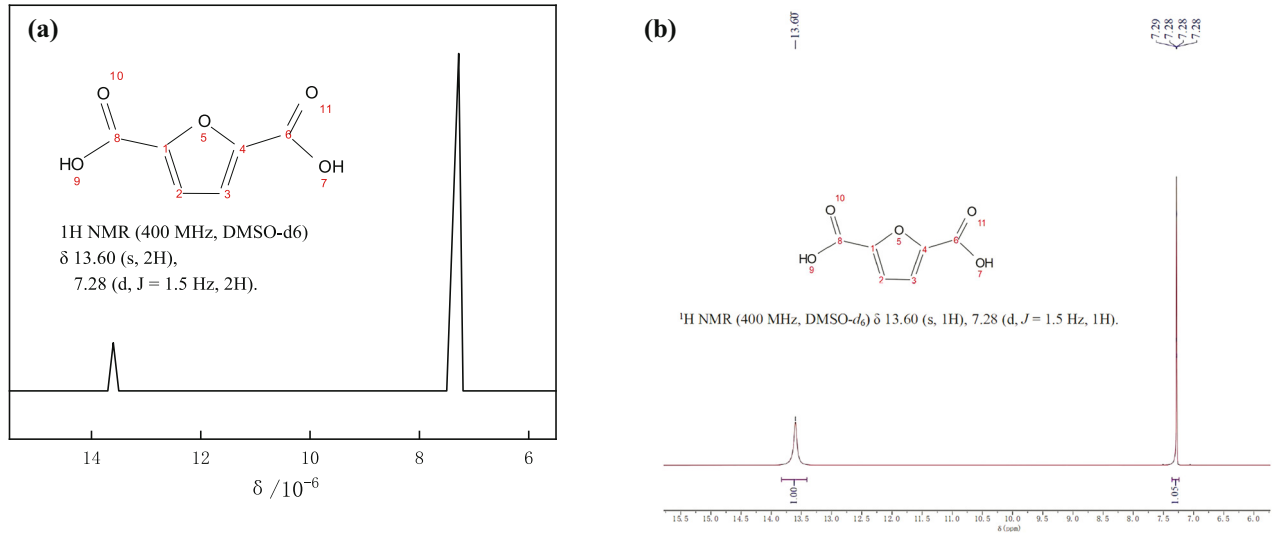

Figure 3: H[1]-NMR spectra of FDCA. Figure 3a is the H[1]-NMR spectra of product. Figure 3b is the H[1]-NMR spectra of standard sample.

and the intermediate cannot be selectively converted to FDCA in time, resulting in polycondensation. At the same time, the side reaction of bromination will also be intensified, resulting in more brominated by-products, reducing the selectivity of FDCA and accelerating the corrosion of the equipment. Moreover, the increases in solvent loss occur because the solvent is susceptible to attack by active radicals or high-valent ions in the Co–Mn–Br catalytic system, triggering the dehydrogenation reaction that generates CO_2 or CO and forming active radicals. Consequently, this leads to the loss of catalytic liquid. Based on the experimental results, a catalytic concentration of 6,200 PPM is deemed more suitable for this study.

3.2 Influence of *n*(Co + Mn)/*n*(HMF) on reaction

The effects of *n*(Co + Mn)/*n*(HMF) on the oxidation products and catalytic liquid loss are shown in Figure 5. From Figure 5, as the concentration of Co and Mn catalysts increases, the

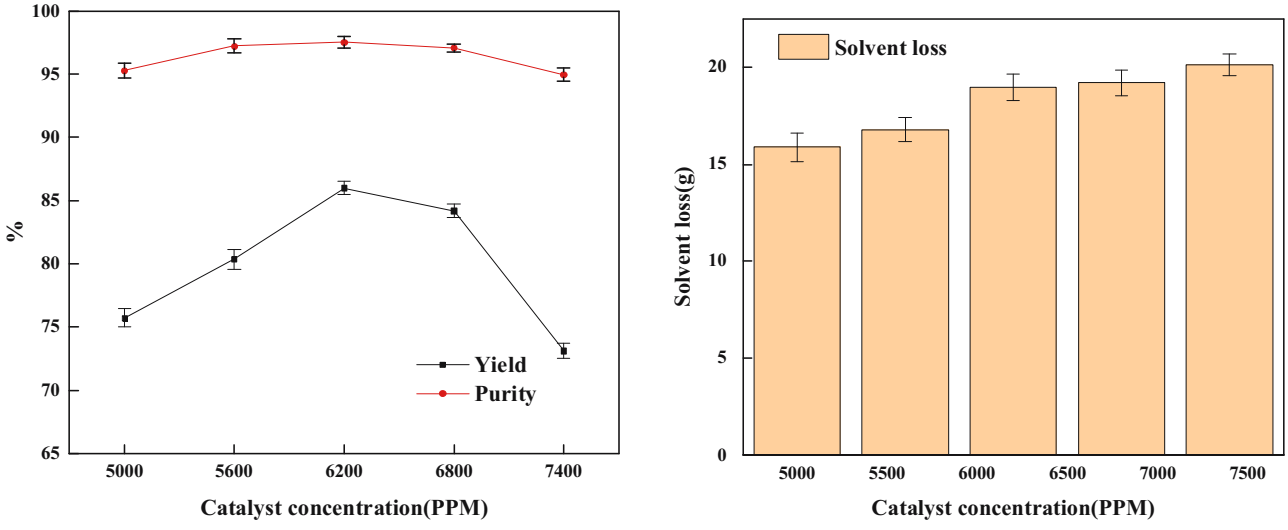

Figure 4: Effect of catalyst concentration on oxidation reaction. (Reaction conditions: *n*(Co)/*n*(Mn)/*n*(Br) = 1/0.04/0.5, *n*(HMF)/*n*(HAC) = 0.05, reaction temperature 170°C, reaction pressure 2 MPa, reaction time 40 min, airflow 1.0 L·min^{-1}).

yield and purity of the product increase first and then decrease, while the loss of the catalytic liquid increases. The liquid-phase oxidation technology of 5-HMF is based on the liquid-phase oxidation technology of *p*-xylene. Both are Co–Mn–Br three-way catalytic systems with HAC as the solvent for air oxidation. There are similarities in the liquid-phase oxidation mechanism between the two processes. In the Co–Mn–Br catalytic system, Co^{2+} is oxidized to Co^{3+} by air, and Co^{3+} acts as a strong oxidant. Similarly, Mn^{2+} is oxidized to Mn^{3+}, with the half-life of Mn^{3+} being much larger than that of Co^{3+}. During the oxidation reaction, Br^- is oxidized to Br·, forming active free radicals and initiating chain reactions.

Therefore, when the concentration of Co and Mn ions is at a low level, the formation rate of high valence metal ions is slow, which affects the whole oxidation reaction rate. As a result, incomplete reactions of the intermediate products occur, leading to the production of by-products and a decrease in yield and purity. The increase in catalytic liquid loss is due to the higher concentrations of the Co and Mn ions. When Co^{3+} oxidizes Mn^{2+}, it will also make the solvent completely oxidized or deeply oxidized to produce CO_2 or CO, thus increasing the solvent loss. Considering industrial production, it is advisable to avoid excessively high concentrations of Co and Mn ions. Therefore, n(Co + Mn)/n(HMF) = 0.173 is more appropriate in this experiment.

3.3 Influence of *n*(Br)/*n*(HMF) on reaction

The effects of n(Br)/n(HMF) on the loss of oxidation products and catalytic liquid are shown in Figure 6. It can be seen from Figure 6 that with the increase in Br concentration, the yield and purity of the product increased first and then decreased, while the loss of the catalytic liquid showed a downward trend. In the Co–Mn–Br catalytic system, Br plays a role in assisting catalysis. Br has a strong hydrogen absorption ability, which can capture the hydrogen on the furan ring and form active free radicals, thus triggering the chain reaction. Therefore, at the beginning of the reaction, a particular concentration of Br ions can promote the smooth progress of the chain reaction so that the substrate HMF can be deeply oxidized. However, when the concentration of Br ions is too high, it is more conducive to the occurrence of bromination side reactions, which ultimately leads to a decrease in the yield and purity of the product. The loss of the catalytic liquid gradually decreased because Co^{3+} was easy to form a complex with Br ions, and electron transfer occurred inside, so that Br ions replaced the acetic acid group and complexed with Co^{3+}, thus slowing down the process of decarboxylation of the acetic acid group. Therefore, n(Br)/n(HMF) = 0.083 is more appropriate in this experiment.

3.4 Influence of reaction temperature on reaction

The effects of reaction temperatures on the loss of oxidation products and catalytic liquid are shown in Figure 7. It can be seen from Figure 7 that as the reaction temperature increases, the product yield first increases and then

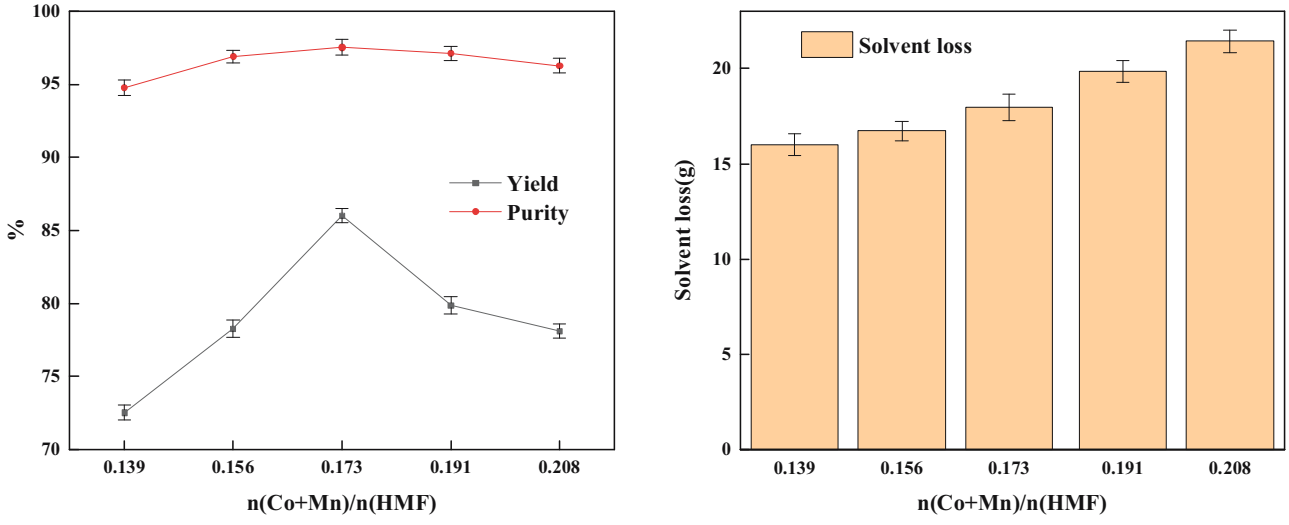

Figure 5: Effect of n(Co + Mn)/n(HMF) on oxidation reaction. (Reaction conditions: n(HMF)/n(HAC) = 0.05, reaction temperature 170°C, reaction pressure 2 MPa, reaction time 40 min, airflow 1.0 L·min^{-1}).

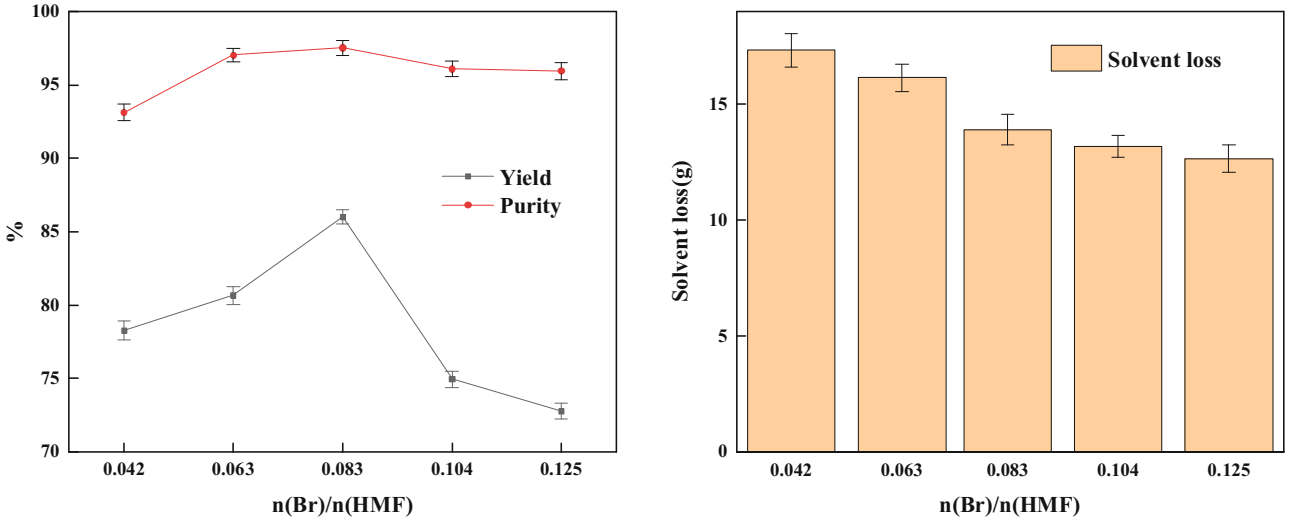

Figure 6: Effect of *n*(Br)/*n*(HMF) on oxidation reaction. (Reaction conditions: *n*(Co)/*n*(Mn) = 1/0.04, *n*(HMF)/*n*(HAc) = 0.05, reaction temperature 170°C, reaction pressure 2 MPa, reaction time 40 min, airflow 1.0 L·min^{-1}).

decreases, while the product purity gradually reaches a stable state. Additionally, the loss of catalytic liquid gradually increases. The oxidation reaction is a free radical reaction, and the reaction temperature significantly influences the activity of the catalyst, which in turn affects the formation of free radicals. Gonzalez-Casamachina et al. [28] found that temperature affected the selective conversion of HMF to FDCA by affecting the formation of free radicals under visible light with O_2 as oxidant and ZnO/PPy as photocatalyst. At lower reaction temperatures, the substrate HMF cannot be converted to the product in time, leading to incomplete oxidation of the intermediate and gradual accumulation, thereby impacting the yield and purity of product. On the other hand, increasing the reaction temperature can accelerate the oxidation of the substrate HMF to FDCA. However, excessively high temperatures can result in deep oxidation of the substrate, resulting in polycondensation side reactions and reduced yield. The increase in catalytic liquid loss is due to the increase in temperature, which accelerates the process of oxidative decarboxylation or decarbonylation of acetic acid. This process contributes to the loss of catalytic liquid. Based on the experimental findings, the reaction temperature of 170°C is considered more suitable for this study, as it strikes a balance between achieving a higher product yield, maintaining product purity, and minimizing catalytic liquid loss.

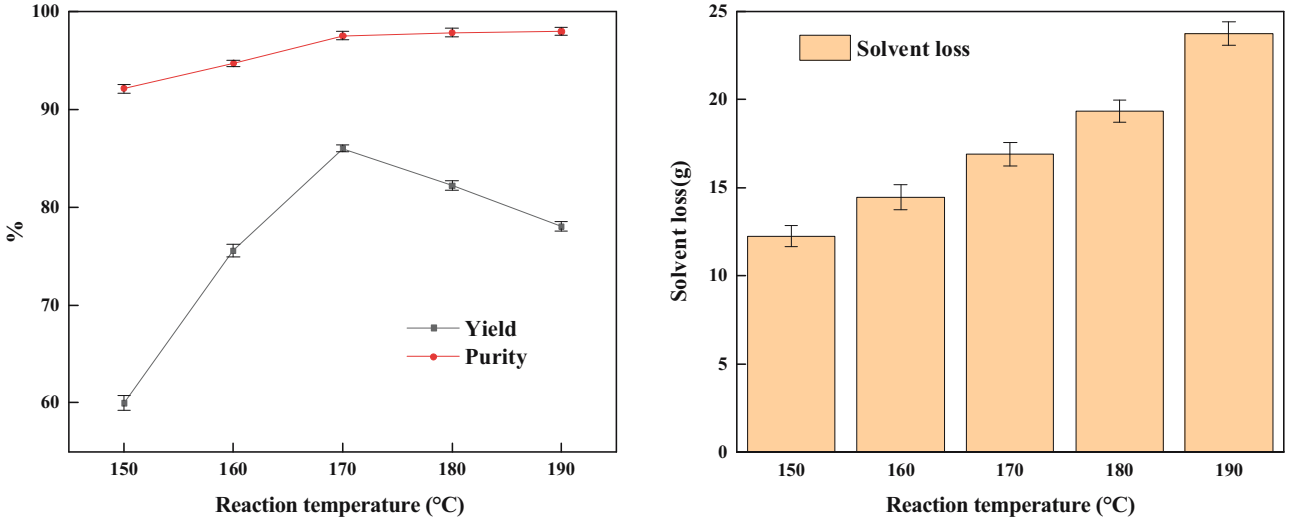

Figure 7: Effect of reaction temperature on oxidation reaction. (Reaction conditions: *n*(Co)/*n*(Mn)/*n*(Br) = 1/0.04/0.5, *n*(HMF)/*n*(HAC) = 0.05, reaction pressure 2 MPa, reaction time 40 min, airflow 1.0 L·min^{-1}).

3.5 Influence of reaction time on reaction

The effects of reaction times on the oxidation products and the loss of catalytic liquid are shown in Figure 8. It can be seen from Figure 8 that as the reaction time increases, the product yield gradually increases to a slight decrease, while the loss of catalytic liquid gradually increases. The oxidation reaction is a series of reactions that require a particular reaction time to complete oxidation. With the increased reaction time, the chain reaction can be carried out smoothly, enabling high selectivity in the oxidation of the substrate HMF.

However, with the increase in reaction time, side reactions become more prevalent, leading to an increase in the possibilities of intermediate polycondensation and excessive oxidation. Consequently, this results in a reduction in the yield and purity of the product. The loss of catalytic liquid demonstrates a steady increase until the reaction time reaches 40 min. After this point, the increase in catalytic liquid loss becomes negligible. This indicates that the oxidation reaction has reached completion, and any further increase in catalytic liquid loss may be attributed to self-combustion. Based on these observations, the reaction time of 40 min is considered appropriate for this experiment. It allows for sufficient reaction time to achieve high selectivity in the oxidation process while minimizing the negative effects of side reactions on product yield and purity. Additionally, it ensures that the oxidation reaction is completed, thus minimizing the loss of catalytic liquid.

3.6 Influence of reaction pressure on reaction

The effect of reaction pressures on the oxidation products and the loss of catalytic liquid is shown in Figure 9. From Figure 9, the yield and purity of the product increased first and then decreased with the increase in reaction pressure, while the loss of catalytic liquid gradually decreased. In the liquid-phase oxidation reaction, when the pressure is low, the dissolved oxygen content in the solvent is low, and the mass transfer resistance of gas–liquid is considerable. Increasing the reaction pressure can enhance the dissolved oxygen concentration in the solvent. Enough oxygen can make the reaction substrate and the intermediate oxidation product more quickly to the substrate for high selective conversion, thus increasing the product's purity. However, with the increase in the reaction pressure, there is also a promotion of oxidation side reactions. These side reactions can lead to undesired outcomes such as the polycondensation reaction of the oxidation intermediate, the ring opening of the furan ring, etc., which result in a decrease in the yield and purity of product. Moreover, excessive high pressure places higher demands on the material of the reactor, which can compromise safety considerations. The increase in reaction pressure makes it easier for the solvent to reach the saturated vapor pressure, slowing down the process of solvent combustion. This is also a contributing factor to the decrease in the loss of catalytic liquid. Under the premise of ensuring the safety of industrial production and maintaining the product's yield

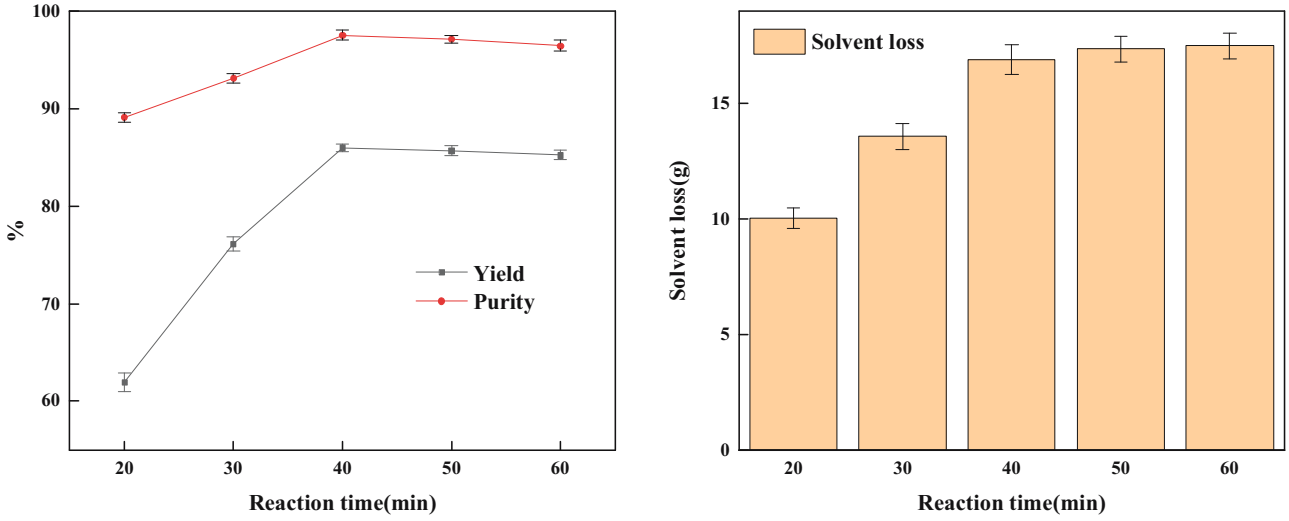

Figure 8: Effect of reaction time on oxidation reaction. (Reaction conditions: *n*(Co)/*n*(Mn)/*n*(Br) = 1/0.04/0.5, *n*(HMF)/*n*(HAC) = 0.05, reaction temperature 170°C, reaction pressure 2 MPa, airflow 1.0 L·min^{-1}).

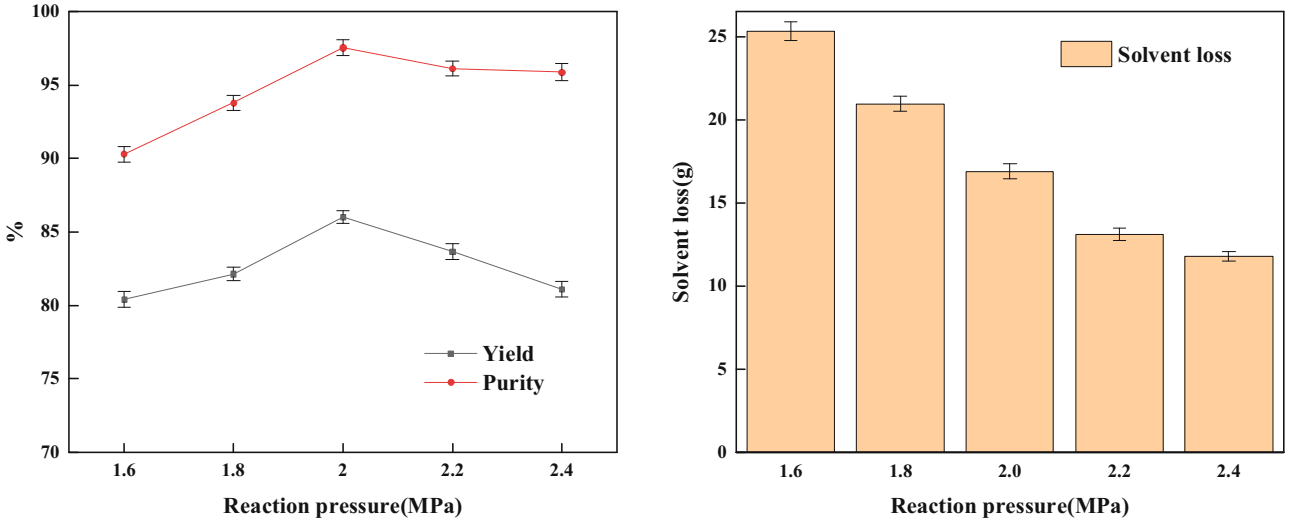

Figure 9: Effect of reaction pressure on oxidation reaction. (Reaction conditions: *n*(Co)/*n*(Mn)/*n*(Br) = 1/0.04/0.5, *n*(HMF)/*n*(HAC) = 0.05, reaction temperature 170°C, reaction time 40 min, airflow 1.0 L·min^{-1}).

and purity, a reaction pressure of 2.0 MPa is deemed more appropriate for this experiment.

3.7 Influence of m(HMF)/m(HAC) on reaction

The effects of solvent ratios on the loss of oxidation products and catalytic liquid are shown in Figure 10. It can be seen from Figure 10 that with the decrease in solvent ratio, the yield and purity of the product increased first and then decreased, while the loss of catalytic liquid gradually decreased. The substrate HMF has high reactivity and is sensitive to reaction temperature and concentration. Under high solvent ratio conditions, HMF is more susceptible to brominated side reactions, polycondensation reactions, and other undesired reactions, which can adversely affect the yield and purity of the product. By reducing the solvent ratio, the instantaneous concentration of substrate HMF is decreased, which in turn reduces the occurrence of brominated side reactions, polycondensation reactions, and other undesired reactions.

However, when the solvent ratio becomes too low, that is, the substrate concentration is very low, a large number

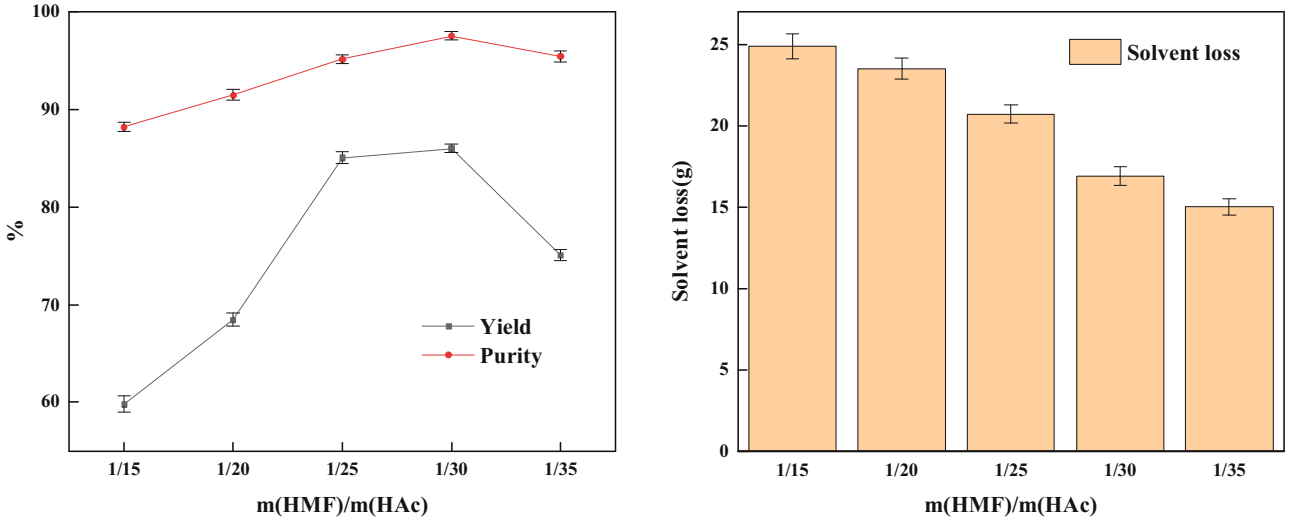

Figure 10: Effect of *m*(HMF)/*m*(HAC) on oxidation reaction. (Reaction conditions: *n*(Co)/*n*(Mn)/*n*(Br) = 1/0.04/0.5, reaction temperature 170°C, reaction pressure 2 MPa, reaction time 40 min, airflow 1.0 L·min^{-1}).

of free radicals attack the furan ring. This can lead to the ring-opening reaction of the furan ring and the generation of additional ring-opening by-products, resulting in a decrease in product yield and purity. Furthermore, while the lower solvent ratio can slow down the combustion of acetic acid, it may also bring about the problem of excessive solvent and increased energy consumption. Considering these factors, the solvent ratio of 1/30 is more appropriate in this experiment.

3.8 Influence of the airflow on reaction

The effect of airflow rates on the oxidation products and catalytic liquid loss is shown in Figure 11. From Figure 11, with the increase in airflow rate, the yield and purity of the product increased first and then decreased slightly, while the loss of catalytic liquid continued to increase. When the airflow rate increases, the amount of oxygen in the reaction also increases. This leads to an improvement in the solubility of oxygen in the catalytic solution and an increase in the gas–liquid-phase interface area, both of which is conducive to improving the oxidation reaction rate.

However, when the airflow rate is too large, the reaction can enter an oxygen saturation state controlled by the reaction kinetics. In this state, the airflow rate has little effect on the reaction rate. Additionally, a high airflow rate reduces the residence time of air in the solvent, which can be detrimental to the reaction process. Furthermore, an increase in airflow can result in the larger amount of solvent being entrained with the exhaust gas. This not only increases the cost of exhaust gas treatment but also leads to a loss of catalytic liquid. Therefore, to ensure that the reaction is not controlled by gas phase mass transfer, it is advisable to carry out the oxidation reaction at a lower airflow rate. In this experiment, an airflow rate of 1.0 L·min^{-1} is more appropriate.

3.9 Influence of catalytic liquid recycling on reaction

In the first three catalytic liquid recycling, the yield and purity of the product were not significantly reduced (Figure 12), indicating that the catalyst system still had an ideal catalytic effect. However, a significant reduction in the yield and purity of the product was observed in the fifth cycle. This can be attributed to the loss of a portion of the Br catalyst during the separation of the FDCA mixture from the solid–liquid.

Although the Co–Mn–Br synergistic catalytic performance is improved by adding 25% Br catalyst during the fourth catalytic liquid recycling, the accumulation of by-product water has a particular impact on the recycling of the catalytic liquid, and multiple reactions also reduce the performance of the catalytic liquid itself, resulting in a decrease in yield and purity of the product. Therefore, under suitable conditions, the catalytic liquid can be recycled multiple times, leading to a reduction in the consumption of precious metal catalysts in the reaction. This recycling capability broadens the scope of industrial application, offering economic and environmental benefits.

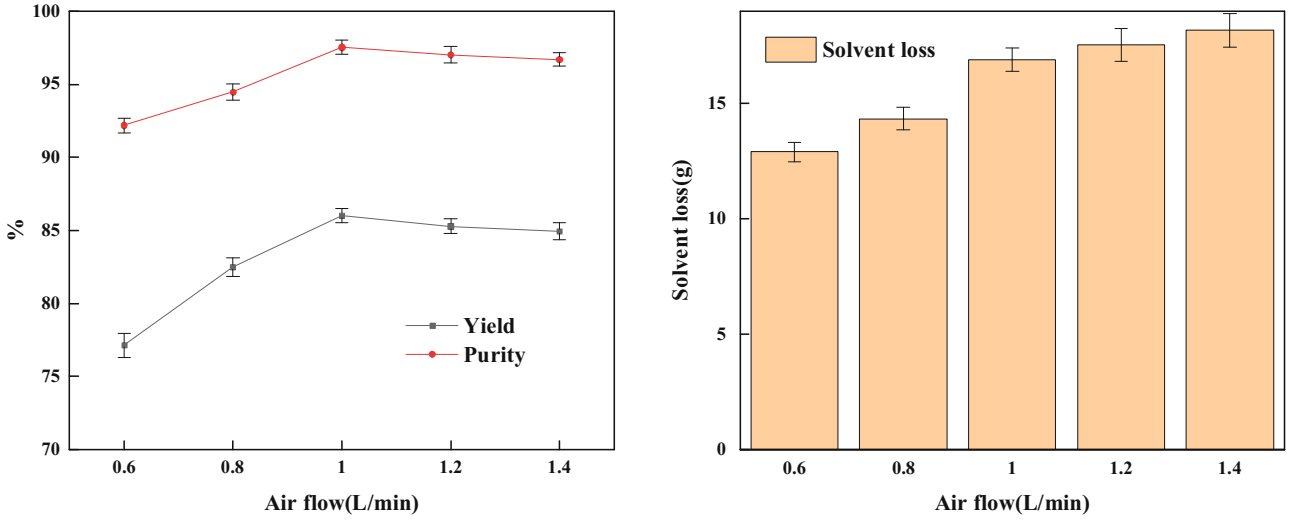

Figure 11: Effect of airflow on oxidation reaction. (Reaction conditions: *n*(Co)/*n*(Mn)/*n*(Br) = 1/0.04/0.5, *n*(HMF)/*n*(HAC) = 0.05, reaction temperature 170°C, reaction pressure 2 MPa, reaction time 40 min).

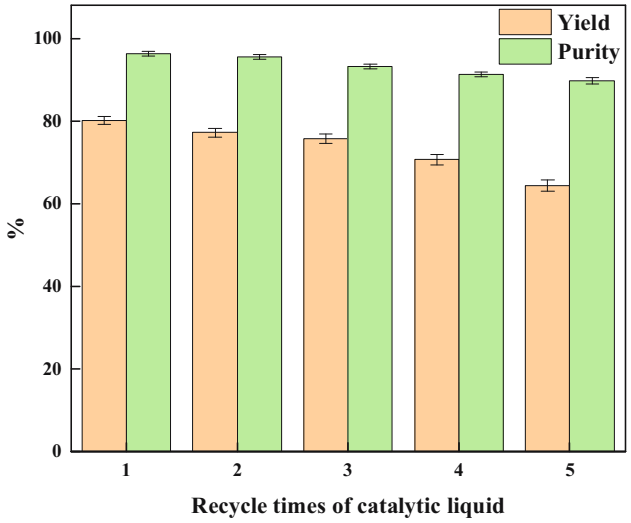

Figure 12: Effect of catalytic liquid recycling on oxidation reaction. (Reaction conditions: *n*(Co)/*n*(Mn)/*n*(Br) = 1/0.04/0.5, *n*(HMF)/*n*(HAC) = 0.05, reaction temperature 170°C, reaction pressure 2 MPa, reaction time 40 min).

4 Liquid-phase oxidation reaction process of HMF

HMF oxidation follows the classical free radical oxidation mechanism and undergoes a chain reaction, generally divided into three stages: chain initiation, growth, and termination. The Co–Mn–Br system acts as a catalyst [29–31], facilitating peroxide decomposition and promoting the formation of free radical. The three catalytic components of Co–Mn–Br with different valence states can increase the rate of electron transfer rate within the chain reaction. These components can cycle between valence states, effectively enhancing the rate of oxidation reaction. Yang and Zhang [32,33] found that charge transfer affects the reduction rate of ions, which affects the selective conversion of substrates to products, and is the rate-determining step affecting the conversion efficiency of HMF.

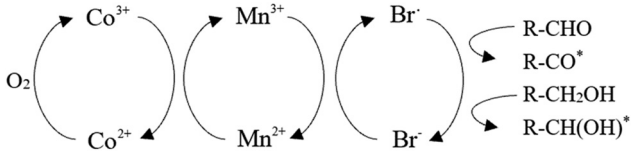

Figure 13: Effect of catalytic liquid recycling on oxidation reaction [34].

During the chain initiation stage, the Co–Mn–Br system undergoes oxidation by air. Specifically, the Co^{2+}–Br complex is oxidized to the Co^{3+}–Br complex by air, while Co^{3+} oxidizes Mn^{2+} to Mn^{3+}. The half-life of Mn^{3+} is much longer than that of Co^{3+}, prolonging the presence of Mn^{3+} in the system. This leads to electron transfer from Br electron, resulting in the generation of bromine radicals. These radicals then capture hydrogen from the hydroxymethyl or aldehyde group of HMF, initiating the formation of free radicals and initiating the chain reaction. At the same time, Co^{2+} can be oxidized to Co^{3+} again. The reaction is repeated throughout the reaction, as shown in Figure 13.

The preparation of furan-dicarboxylic acid catalyzed by catalytic oxidation of the Co–Mn–Br system is a free radical oxidation reaction, mainly involving the oxidation of the hydroxymethyl and aldehyde group to the carboxyl group [34]. The oxidation of HMF to FDCA mainly includes two oxidation processes: alcohol oxidation to aldehyde and aldehyde oxidation to acid. The oxidation process follows the chain reaction mechanism, and the change in catalyst valence state is also coupled with each other until the end of the reaction, as shown in Figure 14.

In the process of HMF oxidation, there are three intermediate products, as shown in Figure 15, which are furan-2,5-dicarbaldehyde (DFF), 5-hydroxymethyl-2-furancarboxylic acid (HMFCA), and 5-formyl-2-furancarboxylic acid (FFCA). The selective conversion of HMF to DFF is significantly more potent than that of HMFCA, indicating that the hydroxymethyl group on the furan ring of HMF has higher activity and is more easily oxidized than the aldehyde group. It is known [35] that the C–H bond dissociation energy on the

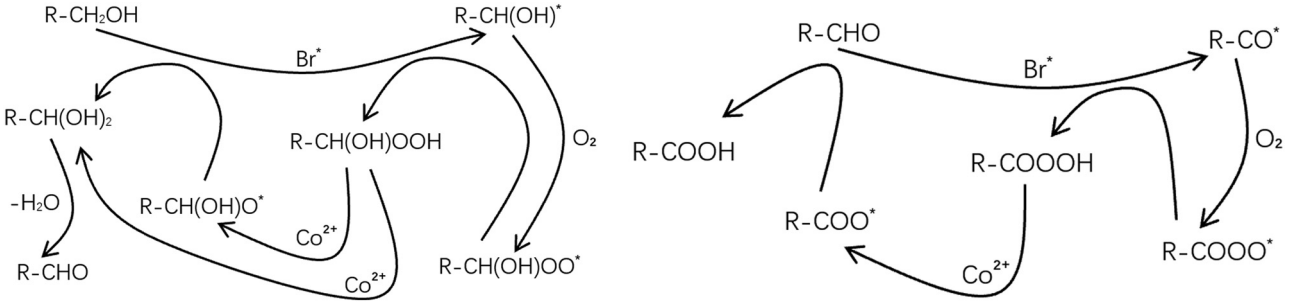

Figure 14: In the process of HMF oxidation, alcohol is oxidized to aldehyde and aldehyde is oxidized to acid [34].

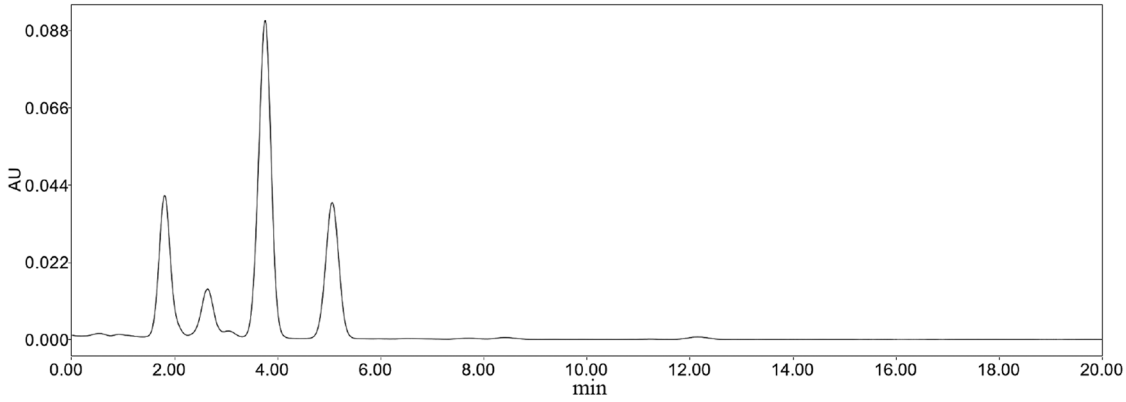

Figure 15: Liquid-phase spectra of FDCA. From left to right are FDCA, HMFCA, FFCA, DFF. (Above experiments were quantitatively analyzed by external standard method. The analysis conditions are as follows: the chromatographic column is a C18 reverse phase chromatographic column; the mobile phase was methanol −0.05% phosphoric acid aqueous solution (volume ratio of 55:45). The flow rate was 0.35 mL·min^{-1}. The detector wavelength was 278 nm. The column temperature was 40°C. The injection volume was 5 μL.).

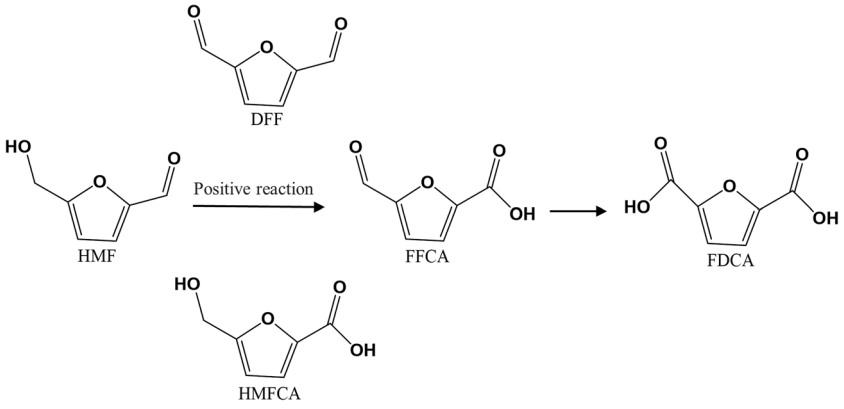

Figure 16: Liquid-phase catalytic oxidation of FDCA.

hydroxymethyl group is 309.8 kJ·mol^{-1}, the O–H bond dissociation energy is 384.1 kJ·mol^{-1}, and the C–H bond dissociation energy on the aldehyde group is 359.7 kJ·mol^{-1}. The C–H bond dissociation energy on the methyl group is much lower than that of the other valence bonds, so the energy required for valence bond cleavage is the lowest, consistent with the result of high-performance liquid chromatography. In summary, this article gives the possible oxidation reaction process of HMF, as shown in Figure 16. This mechanistic understanding of the oxidation process provides insights into the key steps involved in the conversion of HMF to FDCA and the role of the Co–Mn–Br catalyst system in facilitating this transformation.

5 Conclusion

FDCA, a green biomass resource, was prepared by liquid-phase oxidation using HMF as raw material. The catalyst concentration, catalyst ratio, reaction temperature, reaction time, reaction pressure, and solvent ratio were investigated, and the loss of catalytic liquid was analyzed. The product was quantitatively and qualitatively analyzed by liquid chromatography, infrared spectroscopy, and hydrogen nuclear magnetic resonance spectroscopy.

Under the conditions of catalyst concentration 6,200 PPM, n(Co)/n(Mn)/n(Br) = 1/0.04/0.5, n(HMF)/n(HAC) = 0.05, reaction temperature 170°C, reaction pressure 2 MPa, reaction time 40 min and airflow 1.0 L·min^{-1}, FDCA was prepared by liquid-phase oxidation. The final product yield was 86.01%, and the purity was 97.53%. Compared with the existing process [36], this method resulted in an approximately 20% increase in the product yield.

The loss of catalytic liquid under the above oxidation conditions was within a reasonable range, indicating favorable conditions for the recovery and recycling of subsequent catalytic liquid. After the catalytic liquid is recovered, multiple reaction cycles can occur. The yield and purity were

not significantly reduced in the first three reaction cycles. The addition of 25% Br catalyst improved the catalytic performance, and there is a declining trend in product yield and purity. However, the activity of catalyst and the performance of catalytic liquid still decreased over time, impacting the product's yield and purity. Therefore, the catalytic liquid can be recycled many times by adding an appropriate amount of catalyst, which expands the application range for subsequent industrialization.

The oxidation reaction of HMF exhibited a higher reactivity for the hydroxymethyl group compared to the aldehyde group. Therefore, the oxidation reaction primarily occurs in the hydroxymethyl group first. Through analyzing the oxidation reaction intermediates and considering the Co–Mn–Br catalytic mechanism, two possible paths of the HMF oxidation reaction process were speculated: HMF-DFF-FFCA-FDCA and HMF-HMFCA-FFCA-FDCA.

These findings suggest that the liquid-phase oxidation of HMF using the Co–Mn–Br catalyst system is an effective method for the production of FDCA with improved product yield and purity. The study also highlights the potential for recycling the catalytic liquid, thereby reducing the need for additional catalysts and expanding its industrial applicability.

Acknowledgments: This study was financially supported by the National Natural Science Foundation of China (22378026) and The Project of Construction of Innovative Teams and Teacher Career Development for Universities and Colleges under Beijing Municipality (IDHT20180508).

Funding information: Authors state no funding involved.

Author contributions: Linrun Li: writing – original draft, writing – review & editing, methodology, formal analysis; Suohe Yang: software; Haibo Jin: writing – review & editing, resources, funding acquisition, conceptualization; Guangxiang He: writing – review & editing, methodology; Xiaoyan Guo: supervision; Lei Ma: formal analysis, investigation.

Conflict of interest: Authors state no conflict of interest.

Data availability statement: The datasets generated during and/or analyzed during the current study are available from the corresponding author on reasonable request.

References

[1] Arthur J, Ragauskas AJ, Williams CK, Davison BH, Tschaplinski T. The path forward for biofuels and biomaterials. Science. 2006;311(5760):484–9.

[2] Zhu Y, Romain C, Williams CK. Sustainable polymers from renewable resources. Nature. 2016;540(7633):354–62.

[3] Sheldon RA. Green and sustainable manufacture of chemicals from biomass: state of the art. Green Chem. 2014;16(3):950–63.

[4] Basil JN, Ma ADN, Libuse B, Shanks B. Plat-form biochemical for a biorenewable chemical industry. Plant J. 2008;54(4):536–45.

[5] Yuriy R, Juben NC, James AD. Phase modifiers promote efficient production of hydroxymethylfurfural from fructose. Science. 2006;312(5782):1933–7.

[6] Bozell JJ, Petersen GR. Technology development for the production of biobased products from biorefinery carbohydrates-the US Department of Energy's "Top 10" revisited. Green Chem. 2010;28(41):539–54.

[7] Papageorgiou GZ, Tsanaktsis V, Bikiaris DN. Synthesis of poly (ethylene furandicarboxylate) polyesterusing monomers derived from renewable resources: thermal behavior comparison with PET and PEN. Phys Chem Chem Phys. 2014;16(17):7946–58.

[8] Rodriguez DM. 2,5-Furandicarboxylic acid (FDCA)-a very promising building block. Melliand China. 2018;46(10):4–6.

[9] Wang XL, Xie JS, Liao WY. Properties and Applications of Bio-based 2,5-furan Phthalate(FDCA) and Polyester(PEF). Guangdong Chem Ind. 2020;47(7):140–2.

[10] Wu B, Xu Y, Bu Z, Wu L, Li BG, Dubois P. Biobased poly (butylene 2,5-furandicarboxylate) and poly(butyleneadipate-co-butylene 2,5-furandicarboxylate)s: From synthesis using highly purified 2,5-furandicarboxylic acid tothermo-mechanical properties. Polymer. 2014;55(16):3648–55.

[11] Zhou C, Gong DS, Li XM, Bai XS. Synthesis research progress and application prospects of 2,5-furandicarboxylic acid. Dyest Coloration. 2018;55(2):38–42.

[12] Peng W. Study on Melt-spinnability, Fiber Structure and Properties of Poly(ethylene terephthalate-co-ethylene 2,5-Furandicarboxylate) copolyesters. CNKI: Ningbo University; 2018.

[13] Lewkowski J. Synthesis, chemistry and applications of 5-hydroxymethylfurfural and its derivatives. Arkivoc. 2001;34(2):17–54.

[14] Gandini A, Silvestre AJD, Neto CP, Sousa AF, Gomes M. The furan counterpart of poly (ethyleneterephthalate): an alternative material based on renewable resources. J Polym Sci Part A: Polym Chem. 2009;47(1):295–8.

[15] Gandini A, Belgacem MN. Furan chemistry at the service of functional macromolecularmaterials: the reversible Diels-Alder reaction. Oxf Univ Press. 2007;954:280–95.

[16] Fang Z, Smith RL Jr, Qi XH. Production of platform chemicals fromsustainable resources. Biofuels Biorefineries. 2017;9:1659–64.

[17] Meng Y, Huang JS, Li J, Jian YM, Yang S, Li H. Enzyme-mimicking single atoms enable selectivity control in visible-light-driven oxidation/ammoxidation to afford bio-based nitriles. Green Chem. 2023;25:4453–62.

[18] Dijkman WP, Groothuis DE, Fraaije MW. Enzyme-catalyzed oxidation of 5-hydroxymethylfurfural to Furan-2,5-dicarboxylic acid. Angew Chem. 2014;53(25):6515–8.

[19] Li WJ. Synthesis of furan-2,5-dicarboxylic acid and its dimethyl ester catalyzed by ferrous chloride. Chem Reag. 2013;35(8):767–8.

[20] Pan T, Deng I, Xu Q, Zuo Y, Guo QX, Fu Y. Catalytic Conversion of Furfural into a 2,5-Furandicarboxylic Acid Based Polyester with Total Carbon Utilization. Chem Sustainability Energy Mater. 2013;6(1):47–50.

[21] Dick GR, Frankhouser AD, Banerjee A, Kanan MW. A scalable carboxylation route to furan-2,5-dicarboxylicacid. Green Chem. 2017;19(13):2966–72.

[22] Li H, Fang Z, Smith RLJ, Yang S. Efficient valorization of biomass to biofuels with bifunctional solid catalytic materials. Prog Energy Combust Sci. 2016;55:98–194.

[23] Lee JM, Na Y, Han H, Chang S. Cooperative multi-catalyst systems for one-pot organic transformations. Chem Soc Rev. 2004;33:302–12.
[24] Sheldon RA. Atom efficiency and catalysis in organic synthesis. Pure Appl Chem. 2000;72:1233–46.
[25] Janka MJ, Parker KR, Shaikh AS. Oxidation process to produce a crude dry carboxylic acid product. US 8772513; 2014.
[26] Diego Cesar MD, Matheus Adrianus D, Gerardus Johannes Maria G. Method for the preparation of 2,5-furandicarboxylic acid and for the preparation of the dialkyl ester of 2,5-furandicarboxylic acid. US 8865921B2; 2014.
[27] Yutaka K, Miura T, Eritate S. Method of producing 2, 5-furandicarboxylic acid. US 8242292 B2; 2012-08-14.
[28] Gonzalez-Casamachina DA, De la Rosa JR, Lucio-Ortiz CJ, Sandoval-Rangel L, García CD. Partial oxidation of 5 – hydroxymethylfurfural to 2,5-furandicarboxylic acid using O_2 and a photocatalyst of a composite of ZnO/PPy under visible-light: Electrochemical characterization and kinetic analysis. Chem Eng J. 2020;393:124699.
[29] Partenheimer W. The structure of metal/bromide catalysts in acetic acid/water mixtures and its significance in autoxidation. J Mol Catal A: Chem. 2001;174:29–33.
[30] Chavan SA, Halligudi SB, Srinivas D, Ratnasamy P. Formation and role of cobalt and manganese cluster complexes in the oxidation of p-Xylene. J Mol Catal A: Chem. 2000;161:49–64.
[31] Xie G, Cheng YW, Li X. Catalytic mechanism of p-Xylene liquild-phase oxidation. Polyest Ind. 2002;4:1–4.
[32] Yang ZH, Zhang BL, Yan CY, Xue ZM, Mu TC. The pivot to achieve high current density for biomass electrooxidation: Accelerating the reduction of Ni^{3+} to Ni^{2+}. Appl Catal B: Environ. 2023;330:122590.
[33] Zhang YB, Xue ZM, Zhao XH, Zhang BL, Mu TC. Controllable and facile preparation of Co_9S_8–Ni_3S_2 heterostructures embedded with N,S,O-tri-doped carbon for electrocatalytic oxidation of 5-hydroxymethylfurfural. Green Chem. 2022;24:1721–31.
[34] Chen SB. Study on the liquid phase catalytic oxidation process of 5-hydroxymethylfurfural. CNKI: Zhejiang University; 2021.
[35] Heng B, Youdi Z, Shuaibo C, Teng P, Youwei C, Lijun W, et al. Production of 2,5-furandicarboxylic acid by optimization of oxidation of 5-methyl furfural over homogeneous Co/Mn/Br catalysts. ACS Sustain Chem Eng. 2020;8(21):8011–23.
[36] Grushin V, Partenheimer W, Manzer LE. Oxidation of 5-(hydroxymethyl) furfural to 2,5-diformylfuran and subsequent decarbonylation to unsubstituted furan. US 20030055271; 2003.